J. Chem. Sci. (2020) 132:146
https://doi.org/10.1007/s12039-020-01847-5

REGULAR ARTICLE

Copper(II) complexes with semicarbazones: synthesis, characterization and noncovalent interactions in their crystal structures

CLAUDIA C GATTO*, FRANCIELLE C LIMA and PATRÍCIA M MIGUEL
Laboratory of Inorganic Synthesis and Crystallography, University of Brasilia (IQ-UnB), Campus Universitário Darcy Ribeiro, CEP 70904970 Brasília, DF, Brazil
E-mail: ccgatto@gmail.com

MS received 22 June 2020; revised 19 August 2020; accepted 20 August 2020; published online 31 October 2020

Abstract. The present work reports the synthesis and structural elucidation of six novel copper(II) complexes with 2-acetylpyridine semicarbazone (HL^1) and 2-acetylpyridine *N*(4)-phenyl semicarbazone (HL^2). In all compounds, the semicarbazone ligands were find tridentate with *NNO*-donor atoms. The single crystal X-ray diffraction analysis showed the influences of the different copper salt starting reagent in the crystal structures. A packing architectures analysis has been undertaken to delineate the role of relevant noncovalent interactions. The π···π stacking interactions and hydrogen bonds were analyzed using the Hirshfeld surface and fingerprint plots. In addition, the compounds were also characterized by physicochemical and spectroscopic methods.

Keywords. Noncovalent interactions; Crystal structures; Copper(II) complexes; Semicarbazone.

1. Introduction

Polydentate ligands have been extensively investigated to obtain a wide range of compounds with structural diversity and distinct applications. In this context, the use of Schiff bases has been highlighted due to its stability and comprehensive structural versatility.[1–3] The semicarbazones are important for their wide pharmacological profile and constitutive properties that are studied, not only for their chelating capacity when associated with metals in coordination compounds, but also for their comprehensive mechanisms of action. These mechanisms can be specifically predicted by structural description/analysis of the semicarbazones.[4–7]

Commonly the semicarbazones are shown in equilibrium in their keto and enol tautomeric forms, acting as a neutral ligand through the nitrogen atom from the imine group or the oxygen atom from the carbonyl group, or as a monoanionic ligand.[8–10] The structural versatility of semicarbazones is further increased with many possible substituent groups, which most often include new sites of bonding, increasing the possibilities of coordination with metal centers.[2,11] Actually, the diverse structural possibilities of the semicarbazones and their coordination derivatives are responsible for the general applicability of these compounds, which is confirmed by their antiviral, antimicrobial, antiseptic, anti-convulsant, anti-inflammatory and anti-tumor efficacy.[6,12–14]

Additionally, copper complexes have shown satisfactory results regarding the biological activity spectrum.[15–18] Considered one of the most abundant transition metal in the human body, copper is linked to important biological functions, mostly as cofactors of metalloenzymes. The 2+ is the most stable oxidation state for this metal and can form different geometry with semicarbazones ligands.[17,19,20]

Due the our interests in the study of new metallic complexes based on semicarbazones,[21,22] we describe the synthesis and crystal structures of a new ligand, 2-acetylpyridine-semicarbazone (HL^1), and six copper(II) complexes with HL^1 and 2-acetylpyridine *N*(4)-phenyl semicarbazone (HL^2). Their supramolecular arrangements are also discussed herein.

*For correspondence

Electronic supplementary material: The online version of this article (https://doi.org/10.1007/s12039-020-01847-5) contains supplementary material, which is available to authorized users.

2. Experimental

2.1 *Materials and physical measurements*

All reagents and solvents were obtained from commercial sources. HL^2 was prepared as described in the related literature.[23,24] Elemental analyses were performed with Perkin Elmer/Series II 2400 analyzer. Fourier transform infrared spectra were recorded from KBr pellets (4000–400 cm^{-1}) using FT-IR Varian 640. ^1H and ^{13}C NMR spectra were obtained from DMSO-d_6 solutions at room temperature on VARIAN Mercury plus 300 MHz and Bruker Advance III HD 600 MHz spectrometers.

2.2 *X-ray crystal structure analysis*

The X-ray diffraction data were collected on a Bruker CCD SMART APEX II single crystal diffractometer with Mo Kα radiation (0.71073 Å). SADABS was used to scale the data and perform the multi-scan absorption correction.[25] The structures were solved by direct methods using SHELXS-97 and subsequent Fourier-difference map analyses yielded the positions of the non-hydrogen atoms. The refinement was performed using SHELXL-2016.[26,27] Molecular graphics were generated with POV-Ray and DIAMOND programs.[28] The structure of complex 6 contained solvent accessible voids (150 $Å^3$ per unit cell) and SQUEEZE routine in PLATON was used for the disordered solvent molecule.[29] The Table 1 summarizes the crystal data, experimental details and refinement results.

2.3 *Computational details*

The 3D Hirshfeld surfaces (HS) and 2D-fingerprint plots[30,31] were generated with CrystalExplorer 17.5 program,[32] using the crystallographic information files (CIFs). The 3D d_{norm} surfaces (normalized contact distance) were mapped over a fixed color scale of − 0.7148 (red) to 1.2527 (blue). The shape index surface (*S*) was used to verify the π···π stacking interactions, showing color range from − 1.0000 (red) to 1.0000 (blue).

2.4 *Synthesis of $HL^1.HCl.H_2O$*

Semicarbazide hydrochloride (335 mg, 3 mmol) was dissolved in 10 mL of ethanol and mixed with a solution of 2-acetylpyridine (363 mg, 3 mmol) in 5 mL of water. The resulting solution was placed under agitation and reflux for 3 h. After the evaporation of the solvent, single colourless crystals were separated out. Yield: 172 mg (62%). M.p.: 212–214 °C. Elemental analysis: found, C 41.28; H 5.85; N 23.36%; calc. for $C_8H_{13}ClN_4O_2$ (232.67 g), C 41.30; H 5.63; N 24.08%. Selected IR bands (KBr, ν/cm^{-1}): ν(N–H) 3397, 3370, 3300; ν(N–H^+) 3049; ν(N–N) 1116; ν(C=N) 1614, 1600; ν(C=O) 1717. ^1H NMR (H_2O-d_2, 300 MHz, δ ppm from TMS): 2.31 (s, 3 H) 8.00 (t, *J* = 6.6 Hz, 1 H) 8.25 (d, *J* = 8.1 Hz, 1 H) 8.63 (t, *J* = 8.0 Hz, 1 H) 8.73 (d, *J* = 5.5 Hz, 1 H) ppm. ^{13}C NMR (H_2O-d^2, 75 MHz, δ ppm from TMS) 150.3; 127.5; 144.6; 129.2; 149.8; 141.2; 14.34 and 161.3 ppm.

2.5 *Synthesis of 2[Cu(HL^1)Cl_2], (1)*

HL^1 (27.77 mg, 0.1 mmol) was dissolved in 5 mL of ethanol and added to a solution of $CuCl_2$ (13.45 mg, 0.1 mmol) in 5 mL of ethanol. The solution was subjected to shaking at room temperature for 3 h. Green crystals were obtained and were suitable for single crystal X-ray analysis. Yield: 375 mg (60%). M.p.: 232–233 °C. Elemental analysis: found, C 30.67; H 3.05; N 17.46%; calc. for $C_{16}H_{20}Cl_4Cu_2N_8O_2$ (625.28 g) C 30.73; H 3.22; N 17.92%. Selected IR bands (KBr, ν/cm^{-1}): ν(N–H) 3392, 3271; ν(N–N) 1153; ν(C=N) 1599, 1574; ν(C=O) 1661.

2.6 *Synthesis of [{Cu(HL^1)SO_4}]$_2$·$2H_2O$, (2)*

HL^1 (25.43 mg, 0.1 mmol) was dissolved in 5 mL of methanol and was treated with a solution of $CuSO_4$ (15.96 mg, 0.1 mmol) in the same amount of solvent (5 mL of methanol). The solution was subjected to shaking at room temperature for 3 h. Green crystals of salt were obtained after DMF recrystallization. Yield: 106 mg (30%). M.p.: 254 °C. Elemental analysis: found, C 27.85; H 3.44; N 16.70% calc. for $C_8H_{12}CuN_4O_6S$ (355.82) C 27.01; H 3.40; N 15.75%. Selected IR bands (KBr, ν/cm^{-1}): ν(N–H) 3362, 3247; ν(N–N) 1152; ν(C=N) 1600, 1572; ν(C=O) 1668.

2.7 *Synthesis of [{Cu(L^2)Cl}$_2$].($DMF)_2$, (3)*

A solution of HL^2 (25.43 mg, 0.1 mmol) in 5 mL of methanol was treated with a solution of $CuCl_2$ (13.45 mg, 0.1 mmol) in the same amount of solvent (5 mL). The solution was subjected to shaking at room temperature for 3 h. Green crystals of salt were obtained after DMF recrystallization. Yield: 308 mg (63%). M.p.: 181–183 °C. Elemental analysis: found, C 46.53; H 3.93; N 15.47% calc. for $C_{17}H_{20}ClCuN_5O_2$ (425.37 g) C 47.00; H 4.74; N 16.46%. Selected IR bands (KBr, ν/cm^{-1}): ν(N–H) 3426; ν(N–N) 1189; ν(C=N) 1600, 1567; ν(C=O) 1657.

2.8 *Synthesis of [Cu(HL^2)Br_2], (4)*

A solution of HL^2 (25.43 mg, 0.1 mmol) in 5 mL of methanol was treated with a solution of $CuBr_2$ (29.56 mg, 0.1 mmol) in the same amount of solvent (5 mL). The solution was subjected to shaking at room temperature for 3 h. Brown crystals of salt were obtained after DMF

Table 1. X-ray structure data collection and refinement parameters for compounds **HL[1]** and **(1–6)**.

	HL[1]	**(1)**	**(2)**	**(3)**	**(4)**	**(5)**	**(6)**
Empirical formula	$C_8H_{13}ClN_4O_2$	$C_{16}H_{20}Cl_4Cu_2N_8O_2$	$C_8H_{12}CuN_4O_6S$	$C_{17}H_{20}ClCuN_5O_2$	$C_{14}H_{14}Br_2CuN_4O$	$C_{14}H_{14}CuN_6O_7$	$C_{28}H_{26}CuN_8O_2$
Formula weight	232.67	625.28	355.82	425.37	477.65	441.85	570.11
Crystal System	Triclinic	Monoclinic	Monoclinic	Monoclinic	Triclinic	Monoclinic	Triclinic
Space group	*P-1*	$P2_1/c$	$P2_1/c$	$P2_1/c$	*P-1*	*Cc*	*P-1*
a (Å)	7.167(2)	7.152(5)	9.372(2)	15.261(4)	8.063(4)	7.807(10)	8.892(4)
b (Å)	8.620(2)	28.295(5)	14.908(3)	8.245(2)	8.402(3)	14.942(2)	10.209(4)
c (Å)	9.621(3)	11.579(5)	10.045(2)	16.827(5)	12.168(4)	14.536(2)	16.419(7)
α (°)	112.153(2)	90	90	90	92.058(2)	90	106.063(2)
β (°)	100.133(2)	102.674(5)	113.325(10)	114.138(10)	91.013(2)	95.929(10)	91.297(2)
γ (°)	94.175(2)	90	90	90	101.704(2)	90	94.744(2)
V ($Å^3$)	1248.04(6)	2286.1(19)	1288.81(5)	1932.33(9)	802.44(5)	1686.53(4)	1425.95(11)
Z	2	4	4	4	2	4	2
ρ calcd (Mg cm^{-3})	1.444	1.817	1.834	1.462	1.967	1.740	1.328
μ (mm^{-1})	0.344	2.360	1.889	1.289	6.314	1.351	0.805
Reflections collected	9032	24139	16751	18876	13174	10129	31183
Reflections unique/Rint	2102/0.0315	5702/0.0231	3941/0.0210	4808/0.0226	3683/0.0309	4900/0.0178	5919/0.0417
Data/restraints/param.	2102/0/144	5702/0/345	3941/0/191	4808/0/242	3683/0/203	4900/2/270	5919/0/362
Absorption correction	Multi-scan	Multi-scan	Multi-scan	Multi-scan	Multi-scan	Multi-scan	Multi-scan
Max/min transmission	0.930/0.820	1.000/0.883	0.520/0.390	0.789/0.550	0.632/ 0.313	0.840/ 0.700	0.946/ 0.692
Final R indices [$I > 2\sigma(I)$]	0.0569/0.1660	0.0359/0.0865	0.0288/0.0781	0.0294/0.0779	0.0365/0.0891	0.0354/0.0997	0.0460/0.1149
GooF	1.096	1.033	1.023	1.036	1.047	1.067	1.099
Largest diff. peak and hole (e $Å^{-3}$)	0.236/− 0.692	0.357/− 0.442	0.377/− 0.349	0.324/− 0.316	0.642/− 0.467	0.567/− 0.282	0.426/− 0.453

recrystallization. Yield: 234 mg (49%). M.p.: 234–236 °C. Elemental analysis: found, C 35.20; H 2.77; N 11.79% calc. for $C_{14}H_{14}Br_2CuN_4O$ (477.65 g) C 35.20; H 2.95; N 11.73%. Selected IR bands (KBr, ν/cm^{-1}): ν(N-H) 3436, 3270; ν(N-N) 1196; ν(C=N) 1571, 1598; ν(C=O) 1650.

2.9 *Synthesis of [Cu(HL^2)(NO$_3$)$_2$], (5)*

A solution of HL^2 (25.43 mg, 0.1 mmol) in 5 mL of methanol was treated with a solution of $Cu(NO_3)_2$ (24.16 mg, 0.1 mmol) in the same amount of solvent (5 mL). The solution was subjected to shaking at room temperature for 3 h. Green crystals of salt were obtained after DMF recrystallization. Yield: 238 mg (54%). M.p.: 217 °C. Elemental analysis: found, C 38.75; H 3.23; N 18.76% calc. for $C_{14}H_{14}CuN_6O_7$ (441.83 g) C 38.06; H 3.19; N 19.02%. Selected IR bands (KBr, ν/cm^{-1}): ν(N–H) 3443, 3270; ν(N-N) 1193; ν(C=N) 1599, 1571; ν(C=O) 1636.

2.10 *Synthesis of [Cu(L^2)$_2$], (6)*

A solution of HL^2 (25.43 mg, 0.1 mmol) in 5 mL of methanol was treated with a solution of copper(II) acetylacetonate (13.09 mg, 0.05 mmol) in the same amount of solvent (5 mL). The solution was subjected to shaking at room temperature for 3 h. Red crystals of the complex were obtained after DMF recrystallization. Yield: 275 mg (47%). M.p.: 200–202 °C. Elemental analysis: found, C 58.67; H 4.46; N 19.05 calc. for $C_{28}H_{26}CuN_8O_2$ (570.11 g) C 58.99; H 4.60; N 19.65%. Selected IR bands (KBr, ν/cm^{-1}): ν(N–H) 3427, 3239; ν(N–N) 1175; ν(C=N) 1595, 1567.

3. Results and Discussion

3.1 *Synthesis and characterization*

The Schiff bases HL^1 and HL^2 were prepared by the condensation reactions of 2-acetylpiridine with semicarbazide and *N*(4)-phenylsemicarbazide in ethanol, respectively. Colourless crystal suitable for single crystal X-ray analysis were obtained only for HL^1. The synthesis of copper(II) complexes **(1–6)** was performed with different copper salts and HL^1 or HL^2 (Scheme 1). In all complexes the ligands are tridentate coordinated with *NNO*-donor atoms. The mononuclear and dinuclear complexes, **(1)** and **(2)** respectively, contains the neutral form of the ligand HL^1, with μ-oxo from the sulfate ion bridging the metal centers in the complex **(2)**.

Crystals of **(1)** were obtained in the mother solution and crystals of **(2)** after DMF recrystallization. The semicarbazone HL^2 is in deprotonated anionic form in the complexes **(3)** and **(6)**, and in neutral form in the complexes **(4)** and **(5)**. In the compounds, **(3)**, **(4)** and **(5)** the copper atom is coordinated also with Cl^-, Br^- and NO_3^- ions, respectively, originating from the copper salt starting reagent. For the complex **(6)** the acetylacetonate is not present in the crystal structure.

The ^{1}H NMR spectra of HL^1 and HL^2 show proton chemical shifts of the methyl and the pyridine ring. The protons relating to N–H and NH$_2$ had their signals suppressed from the spectrum of HL^1, because they are very labile and were probably exchanged with the deuterium of the solvent, resulting in absence of their signal in the spectrum of the compound. On the other hand, the signals of HL^2 relating to N–H were assigned to 9.97 ppm (s, 1 H) and 9.02 ppm (s, 1 H), to H6 and H7, respectively, between strong electron withdrawing groups. For both HL^1 and HL^2 ligands, the methyl shows a very characteristic singlet signal at the shielded region of the spectrum (2.31 and 2.37 ppm), while the other signals of aromatic protons follow the priority according to the coupling constants (J) cited in literature.[33] The hydrogen atoms marked as 8, 9, 11 and 12 in HL^2 appeared as a singlet at approximately 7.35 ppm, by virtue of being in chemically equivalent environments.[23] The signals of ^{13}C NMR follow the trend, so that the signal of methyl is more shielded and the signal of carbonyl carbon is less shielded, for both ligands. In contrast, as predicted in the literature, the signals of C4 and C2 of HL^1 have become reversed due to the presence of the *N*-carbamoylhydrazone group attached to the pyridine ring, which renders the hydrogen at the position number 4 unshielded in comparison to the hydrogen at position 2. Therefore, the chemical shift ascribed to the carbon at the position 4 (129.2 ppm) is higher than that for the carbon positioned at number 2 (127.5 ppm). The C5 is assigned to 149.8 ppm, being less shielded than carbon of the imine (C6), since it undergoes the inductive effect of two directly attached groups that withdraw electrons.[34,35] The carbons in the phenyl ring of HL^2 are assigned accordingly to the similarity between them, thus C10 and C14, as C11 and C13, are located in chemically equivalent environments and are therefore regarded as chemically identical.[24] The ^{1}H and ^{13}C NMR spectra are in Supplementary Information (Figures S15–S18).

In the IR spectra, it was not possible to observe Cu–O/Cu–N, due the generally frequencies of these bonds have low energy vibration and therefore appear in a lower region of characteristic wavenumber, ν(Cu–O) in 335–530 cm^{-1} and ν(Cu–N) in 360–440 cm^{-1}. We observed ν(C=O) equals to 1717 cm^{-1} for HL^1 and 1683 cm^{-1} for HL^2. As the coordination of copper(II)

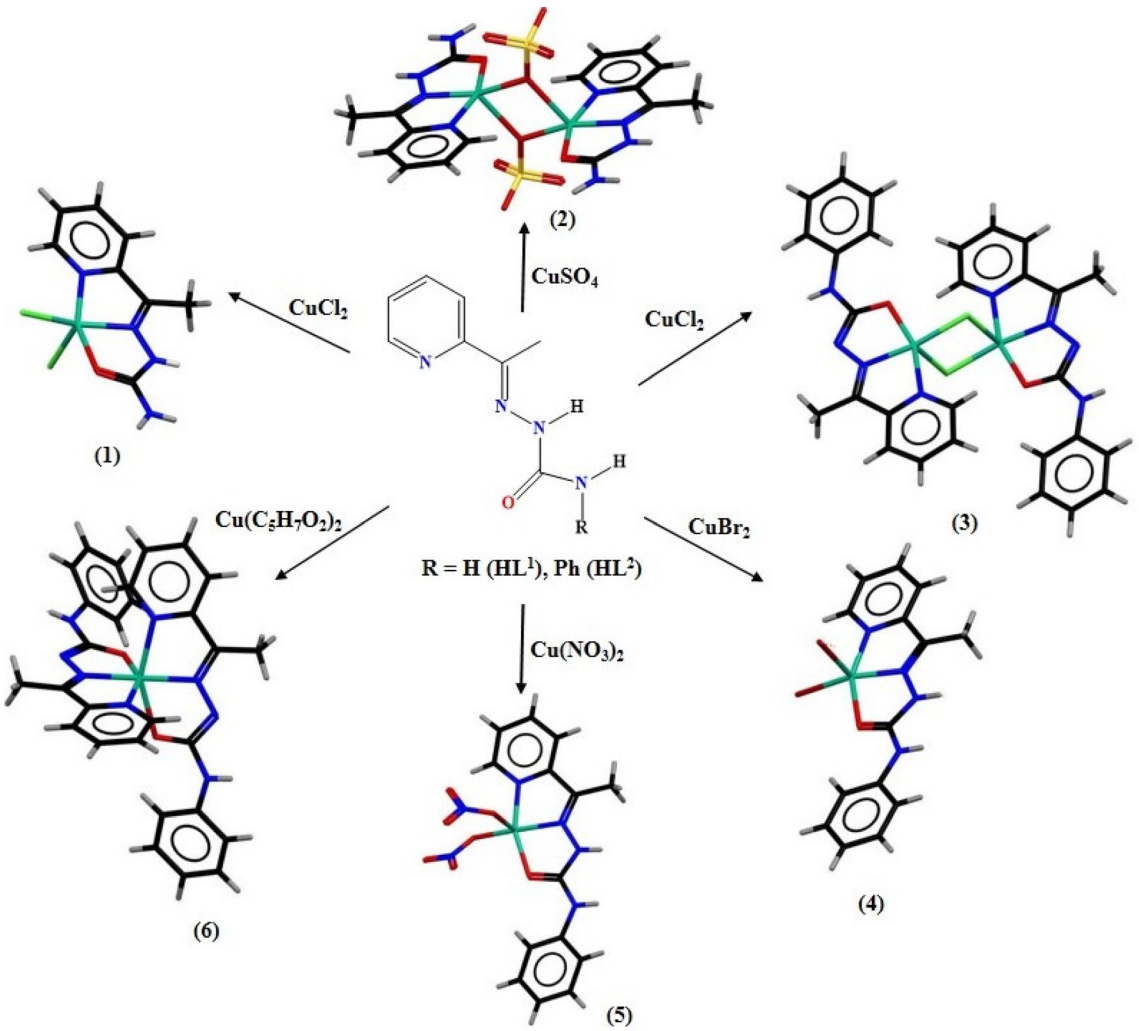

Scheme 1. Semicarbazone ligands (HL^1 and HL^2) and their copper(II) complexes **(1–6)**.

atom with the semicarbazone is shifted to lower wavelength values, the strength of the connection C=O decreases. The ν(C=O) of the complexes are observed at 1661 cm^{-1} for **(1)**, 1668 cm^{-1} for **(2)**, 1657 cm^{-1} for (3), 1650 cm^{-1} for **(4)** and 1636 cm^{-1} for **(5)**.[33] In contrast, for **(6)** there was an absence of this band stretching, with the appearing of a stretching band ν(C–O) of 1231 cm^{-1}, which suggests the loss of strength by the double bond due the coordination with the metal center. Analogous situation occurred to the band of stretch ν(C=N), which moved for the lower values of wavenumber, also due the coordination to the metal in this site of the ligand.[36] However, a compression was observed in the bonds of the imine, whose lengths are 1.295(3) Å for HL^1, 1.283(3) Å for **(1)** and 1.287(3) Å for **(2)**. This effect is explained due that the bond to the copper atom increases the effective mass and leads to a decrease in the reduced mass, which reduce the stretching energy, even though the bond length is shorter. The vibration frequency related for ν(NH^+) deriving from pyridine protonation, which occurs only in the free ligand, was observed at 3049 cm^{-1} in HL^1 and 2920 cm^{-1} in HL^2.

The presence of ν(SO_4^{2-}) for **(2)** at 951, 1114 and 1185 cm^{-1} confirms the bidentate form of the complex with copper(II) atom, which is consistent with values found in literature for symmetric and asymmetric displacements, since the absorption band related to the sulfate coordinated in monodentate form usually appears shifted to lower wavelength values.[33, 37] In **(5)**, the presence of the bands relating to stretches of nitrate ion appeared at 1490, 1298, 1016 and 763 cm^{-1}, according to data found in literature.[33,34]

3.2 *Crystal Structure Description*

After the synthesis and single crystal X-ray diffraction analysis seven new structures were obtained of the

compounds: $HL^1 \cdot HCl \cdot H_2O$, $2[Cu(HL^1)Cl_2]$ **(1)**, $[\{Cu(HL^1)SO_4\}]_2 \cdot 2H_2O$ **(2)**, $[\{Cu(L^2)Cl\}_2] \cdot (DMF)_2$ **(3)**, $[Cu(HL^2)Br_2]$ **(4)**, $[Cu(HL^2)(NO_3)_2]$ **(5)** and $[Cu(L^2)_2]$ **(6)**.

The structural analysis of compound HL^1 (Figure 1) showed the ketone form with a typical double-bond C8=O1 of 1.223(3) Å, in accordance with a similar structure with related bond length of 1.223(3) Å.[38] The bond angles between 114.0(2)° and 126.3(3)° along the semicarbazone chain almost confer planarity for the molecule and are justified by sp^2 hybridization of the nitrogen atoms, with trigonal planar geometry and torsion angles of − 79.8(2)° for the side arm C6–N2–N3–C8. The oxygen atom O1 and the hydrazone nitrogen N2 are in the *E* configuration with respect to the C8–N4 bond. The results of X-ray diffraction analyses also indicated an extended π-delocalization throughout the semicarbazone, in which the N2–N3 bond length is 1.353(3) Å and the N4–C8 is 1.332(3) Å, both between the ideal values corresponding to single and double bonds.[24] The structure of HL^1 is comprised of a protonated semicarbazone cation, a Cl anion and one water molecule of crystallization that stabilize the crystal lattice through a network of relevant noncovalent interactions. The Cl^- is stabilized by two intramolecular hydrogen bond between N4–H4B···Cl1 and with the protonated N-pyridyl atom, N1–H1A···Cl1. Others intra and intermolecular hydrogen bonds were observed, Table 2. Interestingly, all these noncovalent interactions in HL^1 form an infinite one-dimensional network and are responsible for the formation of a supramolecular arrangement (Figure S1 in SI).

The complex **(1)** shows two independent molecules in the unit cell and the metal centers are coordinated with the neutral semicarbazone HL^1 in tridentate form and with two chloride ions (Figure 1). A similar structure with 2-benzoylpyridine-semicarbazone ligand was reported, as well as a related dimer coordinated by bridges of chloride ions with 2-acetylpyridine-semicarbazone.[9, 23]

The Addison's parameter (τ) was used to predict the pentacoordinated polyhedron in complex **(1)**.[39] The τ value is defined by $|\beta - \alpha|/60$, where β and α are the *trans* angles of the polyhedron's base. For the perfect trigonal bipyramid geometry, the τ value should be one, and zero for the perfect square pyramid geometry. The calculated Addison's parameters for the two monomeric units were 0.179 and 0.097, indicating square pyramid distorted geometry for both copper atoms.[40] The bond angles Cl–Cu–Cl of 102.64(3)° and 103.64(3)°, and bond lengths Cu–Cl are between 2.197(8) Å and 2.583(2) Å, and are comparable to the corresponding values of other similar compounds.[19,36] The crystal structure of **(1)** shows the semicarbazone molecule in keto tautomerism and in the *Z*-isomeric form due to the placement of the azomethine nitrogen N2 in respect to the oxygen atom O1 *cis*. The bond length C=O reported for HL^1 is 1.223(3) Å and is lengthened to 1.253(3) Å and 1.250(3) Å on copper coordination, which is typical of a ketone form with concomitant shortening of terminal C–N bond of

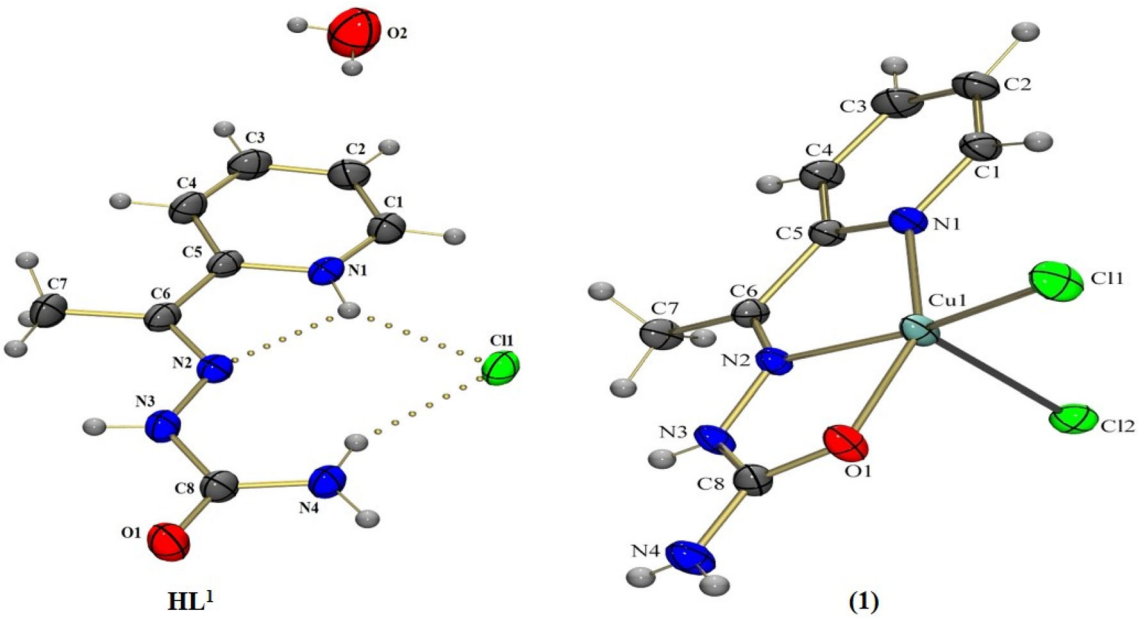

Figure 1. Molecular structures of $\mathbf{HL^1}$ and **(1)** with crystallographic labelling. Thermal ellipsoids with 30% of probability.

Table 2. Hydrogen bonding interactions (Å and °) for **HL[1]** and **(1)**–**(6)**.

Compound	D–H···A	d(D–H)	d(H···A)	d(D···A)	(D–H···)
HL[1]	N1–H1A···N2	1.05(5)	2.11(4)	2.635(4)	108(3)
	N1–H1A···Cl1	1.05(5)	2.23(5)	3.062(2)	135(3)
	N4–H4B···Cl1	0.86	2.46	3.266(3)	155.7
	N4–H4A···Cl1^{i}	0.86	2.54	3.349(3)	157.1
	N3–H3A···O1^{ii}	0.86	2.54	3.349(3)	157.1
1	N(7)–H(7)···Cl(4)^{iii}	0.81(3)	2.40(3)	3.117(3)	149(3)
	N(3)–H(3A)···Cl(2)^{iv}	0.75(3)	2.40(3)	3.108(2)	157(3)
	N(4)–H(4B)···Cl(2)^{iv}	0.78(3)	2.59(3)	3.293(3)	152(3)
	N(4)–H(4A)···O(2)^{v}	0.84(3)	2.23(3)	3.032(3)	160(3)
	N(4)–H(4A)···Cl(3)^{v}	0.84(3)	2.83(3)	3.380(3)	125(3)
	N(8)–H(8A)···O(1)^{v}	0.79(4)	2.37(4)	3.073(3)	150(3)
	N(8)–H(8A)···Cl(1)^{v}	0.79(4)	2.83(4)	3.430(3)	135(3)
	N(8)–H(8B)···Cl(4)^{iii}	0.84(4)	2.59(4)	3.323(2)	146(3)
2	O(6)–H(6A)···O5^{vii}	0.77	2.07	2.831(3)	168.1
	O(6)–H(6B)···O4^{viii}	0.69	2.07	2.755(2)	169.1
	N(3)–H(3A)···O5^{vi}	0.84(2)	1.85(2)	2.689(2)	175(2)
	N(3)–H(3A)···S1^{vi}	0.84(2)	2.95(2)	3.712(2)	151.7(2)
	N(4)–H(4A)···O6^{v}	0.86	1.93	2.783(2)	174.5
	N(4)–H(4B)···O3^{vi}	0.86	2.00	2.848(2)	170.1
	N(4)–H(4B)···S1^{vi}	0.86	2.89	3.699(2)	157.7
4	N(4)–H(4A)···Br2^{ix}	0.86	2.61	3.410(3)	154.6
	N(3)–H(3A)···Br2^{ix}	0.95(4)	2.37(4)	3.235(3)	152(3)
5	N(4)–H(4A)···O4^{x}	0.86	2.24	3.054(5)	158.3
	N(3)–H(3A)···O3^{x}	0.86	1.95	2.761(5)	156.7
6	N(4)–H(4A)···N7^{xi}	0.75(3)	2.37(3)	3.111(4)	173(3)
	N(8)–H(8A)···N3^{xii}	0.85(3)	2.16(4)	3.007(4)	177(3)

Symmetry transformations: (i) 2 – x, 2 – y, 1 – z; (ii) 1 – x, 1 – y, – z; (iii) – x + 1, – y, – z + 1; (iv) x, – y + 3/2, z – 1/2; (v) – x + 1, – y + 1, – z + 1; (vi) x, – y + 1/2, z + 1/2; (vii) – x + 1, – y + 1, – z; (viii) x + 1, y + 1, z; (ix) 1 – x + 1, – y + 2, – z + 2; (x) x – 1/2, y – 1/2, z; (xi) x – 1, y, z; (xii) x + 1, y, z.

1.332(3) Å to 1.318(4) Å and 1.322(4) Å. Both monomeric units of the complex **(1)** are strongly linked by several N–H···Cl and N–H···O intermolecular interactions in the crystal lattice and are involved in the formation of corrugated layers by means to form a supramolecular structure (Figure S2 in SI). The π···π stacking interactions between two pyridyl ring is observed in the structure of **(1)**, leading to one dimensional infinite chains, with centroid-centroid distance of 3.533(2) Å (Figure 2).

The compound **(2)** shows two sulfate anions in the structure making bridges between the two copper atoms and two coordinated molecules of HL^1 semicarbazone (Figure 3). Each ligand molecule is the keto tautomer and *E* isomer coordinated to a copper atom. Unlike what is presented by Layana *et al.*,[41] where the presented dimer is composed of metallic centers of different geometries, and by Lee *et al.*,[42] in which the ligand itself bridges the metals, here each metallic center is pentacoordinated with *N*-pyridyl nitrogen (N1), nitrogen azomethine (N2), oxygen enolate (O1) semicarbazone and two oxygen atoms (O2, O2′) of the sulfate group.

The Addison's parameter is 0.103 and shows that each Cu(II) atom gives a square pyramid distorted geometry, while the O2 atom of the sulfate anion occupied the apical position.[39] The Cu–Cu distance in the dimeric complex **(2)** is 3.293 Å, long enough to not exist Cu···Cu interaction. The bond lengths Cu1–N1 of 1.997(2) Å, Cu1–N2 of 1.937(1) Å and Cu1–O1 of 1.978(1) Å are provided in accordance with other copper complexes.[8] The polyhedrons formed are distorted with bond angles formed by the atoms of the base ranging from 79.94(6)° to 166.16(6)°. In the complex **(2)** a series of noncovalent interactions were formed. Intermolecular hydrogen bonds involving N3 and N4 atoms, the sulfate group and the water molecule of crystallization were observed (Table 2). Intermolecular hydrogen bonds that involve solvent water molecule serves as double donor and single

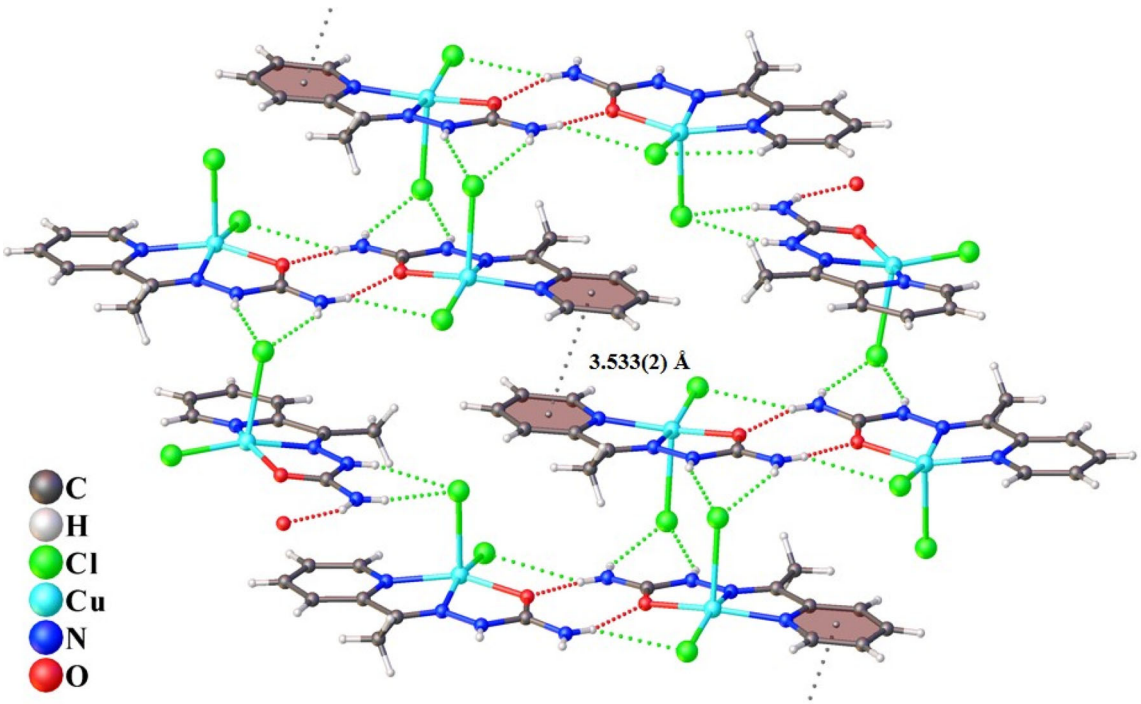

Figure 2. View of **(1)** showing the 1D chain made up of π···π stacking interactions and hydrogen bonds.

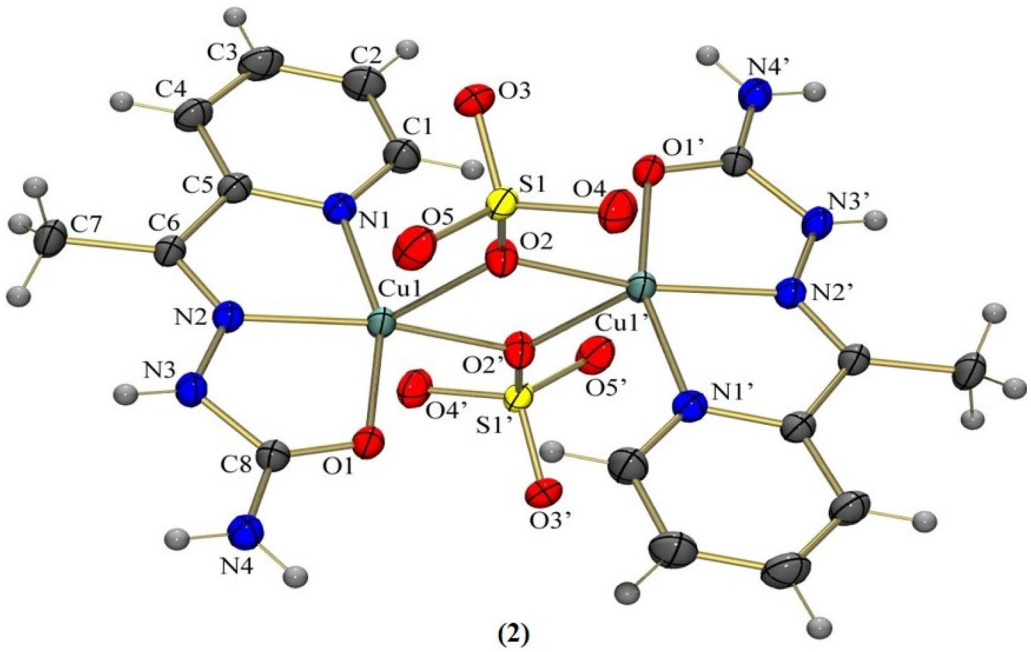

Figure 3. An ORTEP representation (30% probability displacement ellipsoids) of the complex **(2)**. Symmetry operations (′): 1 − x, − y, 1 − z.

acceptor connect the neighboring layers in the third dimension (Figure S3 in SI). Selected bond lengths and angles for HL^1, **(1)** and **(2)** are depicted in Table S2 (SI).

The molecular structure of **(3)** show a binuclear compound with monoanionic and *NNO*-tridentate semicarbazone and two chloride ions bridging the copper(II) centers in an axial-equatorial position

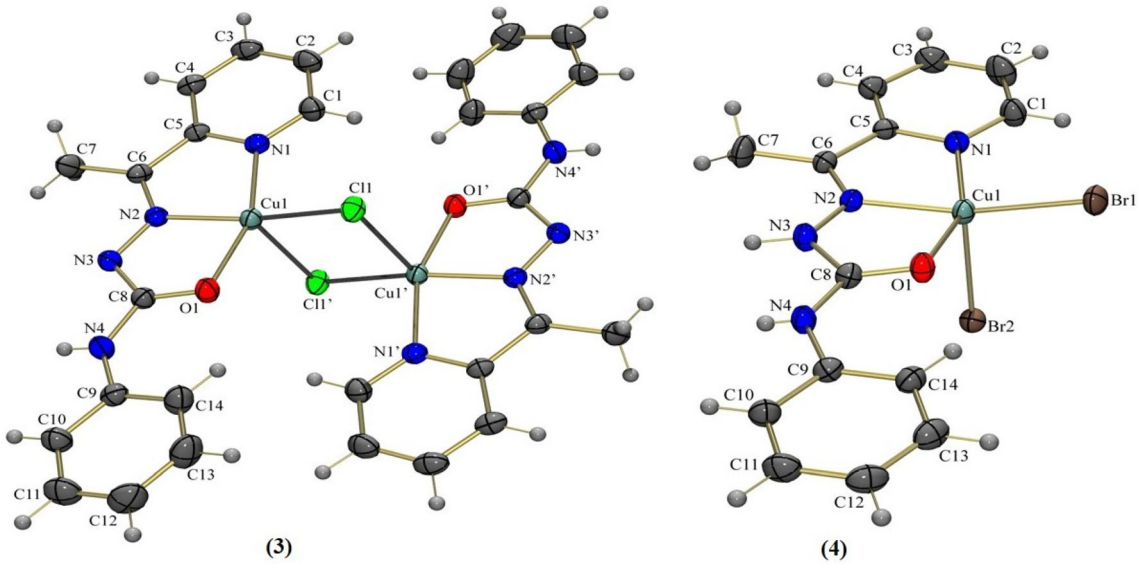

Figure 4. Molecular structures of **(3)** and **(4)** with crystallographic labelling. The thermal ellipsoids are drawn at 30% probability level.

(Figure 4). The bond angle between Cl1–Cu1–Cl1 is 90.805(2)° and the equatorial bond length Cu1–Cl1 is 2.243(5) Å, [symmetry operations: − x + 1, − y + 1, − z + 1], much shorter than the corresponding axial Cu1–Cl1 distance of 2.639(5) Å. Each copper atom in **(3)** show a distorted square pyramid geometry with Addison's parameter τ of 0.114.[39] In addition, the Cu–Cu distance of 3.439(1) Å indicates to be long enough to preclude any metal–metal interaction. This distance is longer than the Cu–Cu distance of 3.293 Å found in the complex **(2)**.[43] A comparison among the mononuclear **(1)** and binuclear **(3)** compounds, showed shorter bond distances Cu–Cl and longer bond distances Cu–N and Cu–O in **(1)** than the corresponding bonds distances in **(3)**, probably due the formation of the bridge between the metal centers with the chloride ions. The bond distances C6–N2, N2–N3, N3–C8 and C8–O1 in **(3)** show substantial evidence of electron delocalization on the ligand around the coordination sphere, since they have intermediate character between single and double bonds. This compound also presents two DMF molecules as solvent of crystallization and no π···π stacking interactions and hydrogen bonds were found in this compound. Selected bond distances (Å) and bond angles (°) for **(3)** are in Table S3 (SI).

The complex **(4)** show the metal center coordinated by neutral tridentate ligand and two bromide ions (-Figure 4). The copper(II) atom features a distorted square pyramid geometry with Addison's parameter τ of 0.145.[39] Differently of the binuclear complex **(3)**, to the mononuclear complex **(4)**, the bromide ions not act as a bridge compared with chloride ions, probably due the volume of the halogen atoms. Similar compounds with copper(II) atoms and 2-benzoylpyridine-phenylsemicarbazone were reported in the literature.[44] The equatorial bond length Cu1–Br1 of 2.336(6) Å is much shorter than the corresponding axial distance Cu1–Br2 of 2.651(6) Å. In **(4)** intermolecular interactions give a bifurcated arrangement and reveal the formation of a dimer, connecting two molecules of the compound through hydrogen bonds (as shown the Figure S4 in SI).

An ORTEP drawing of the molecular structure of the complex **(5)** is depicted in Figure 5. The copper(II) is coordinated by neutral tridentate ligand and two nitrate ions. The crystal structure of **(5)** shows the semicarbazone molecule in the *Z*-isomeric form, due to the *cis* placement of the oxygen atom O1 to the azomethine nitrogen N2 in keto tautomer. The metal atom is coordinated by the *N*-pyridyl and azomethine nitrogenin *cis* position. The coordination environment around the copper(II) atom is best described as five-coordinated: the O2 atom is located in the apical position of the distorted square pyramid geometry, wherein the atoms N1, N2, O1 and O5 constitute the square with slight displacement. This structure has a calculated Addison's parameter τ equals 0.0005.[39] The apical copper-nitrate bond of 2.374(3) Å is longer than the in-plane copper-nitrate bond of 1.925(3) Å, due the repulsion along the *z* axis with the presence of two electrons in the dz^2 orbitals. The bond length of Cu1–N1 is 1.992(3) Å and for Cu1–N2 is 1.947(2) Å. The angle N1–Cu1–N2 is 79.91(9)° and is very close to the values described by the related structure.[21] Also a comparison of the main lengths and bond angles with a

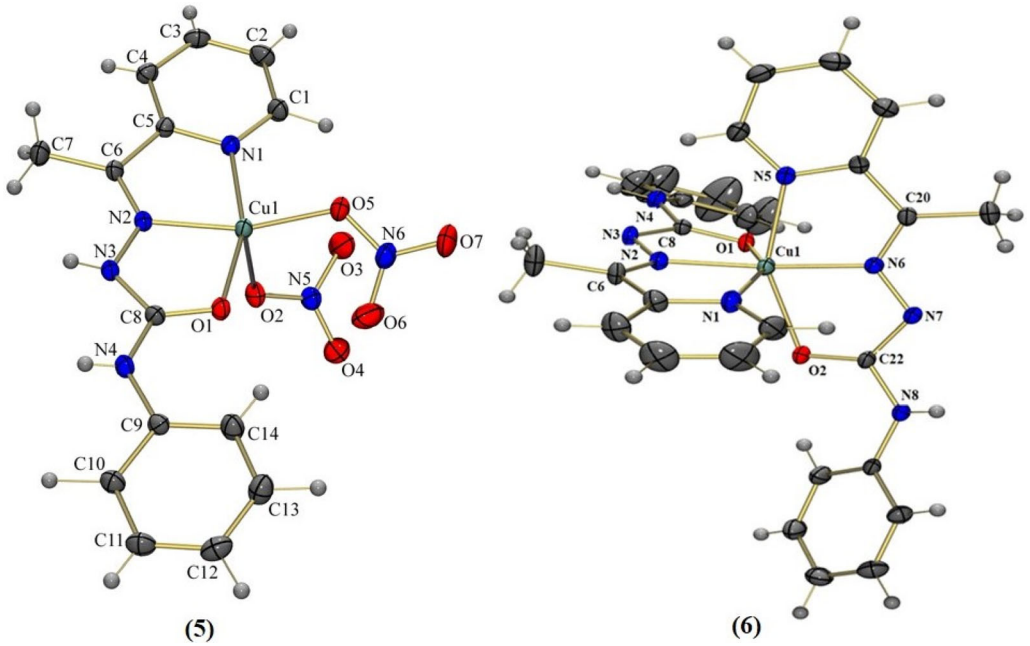

Figure 5. Molecular structures of **(5)** and **(6)** with crystallographic labelling. The thermal ellipsoids are drawn at 30% probability level.

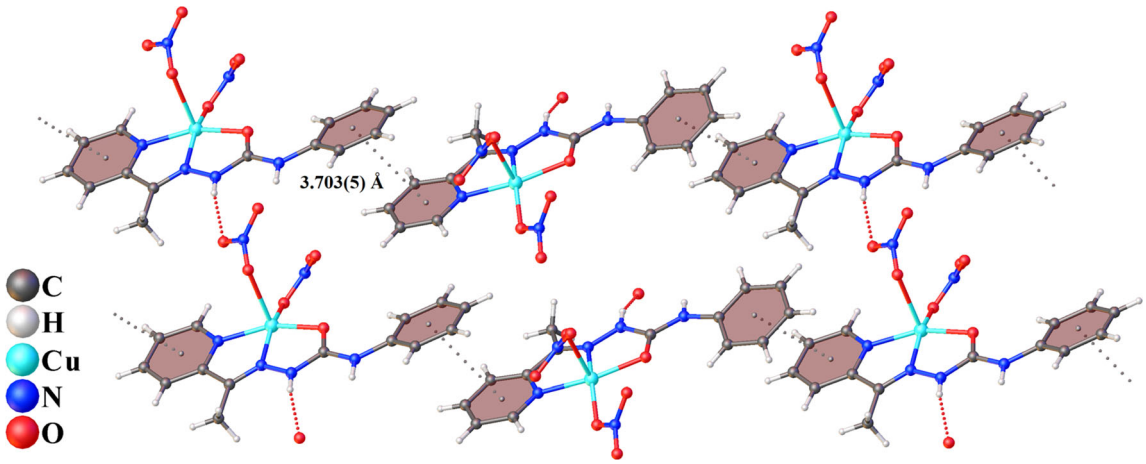

Figure 6. Part of the crystal structure of **(5)** showing the noncovalent interactions.

similar structures reported shows concordance with the synthesized complex.[45] Intermolecular hydrogen bonds are observed and are associated with the formation of a one-dimensional network in the crystallographic plane *bc* (Figure S5 in SI). The π···π stacking interactions also were observed between the phenyl groups in **(5)**, with centroid-centroid distance of 3.703(5) Å (Figure 6).

In the structure of complex **(6)**, the copper(II) atom is coordinated by two monoanionic and tridentate ligand L^2 in a distorted octahedral coordination environment (Figure 5). The bond angles between copper(II) and the semicarbazone are between 75.69(9)° and 173.63(11)°, as observed in a similar Cu(II) complex reported in literature.[46] In addition, for reported complex $[Cu(HL^2)_2](ClO_4)_2$, besides the presence of two perchlorate ions, the differences observed consist of the carbonyl group positions in cis and trans, compared with **(6)**.[38] The bond distances Cu–O of the carbonyl group of 2.212(2) Å and 2.215(2) Å are longer compared to the same bonds in the complexes **(3–5)**. A variation of the π-system distances of the semicarbazone is observed in the bond lengths of the backbone of the ligand, with the N3 and N7 deprotonated nitrogen atoms, at the coordination with Cu(II) atom.

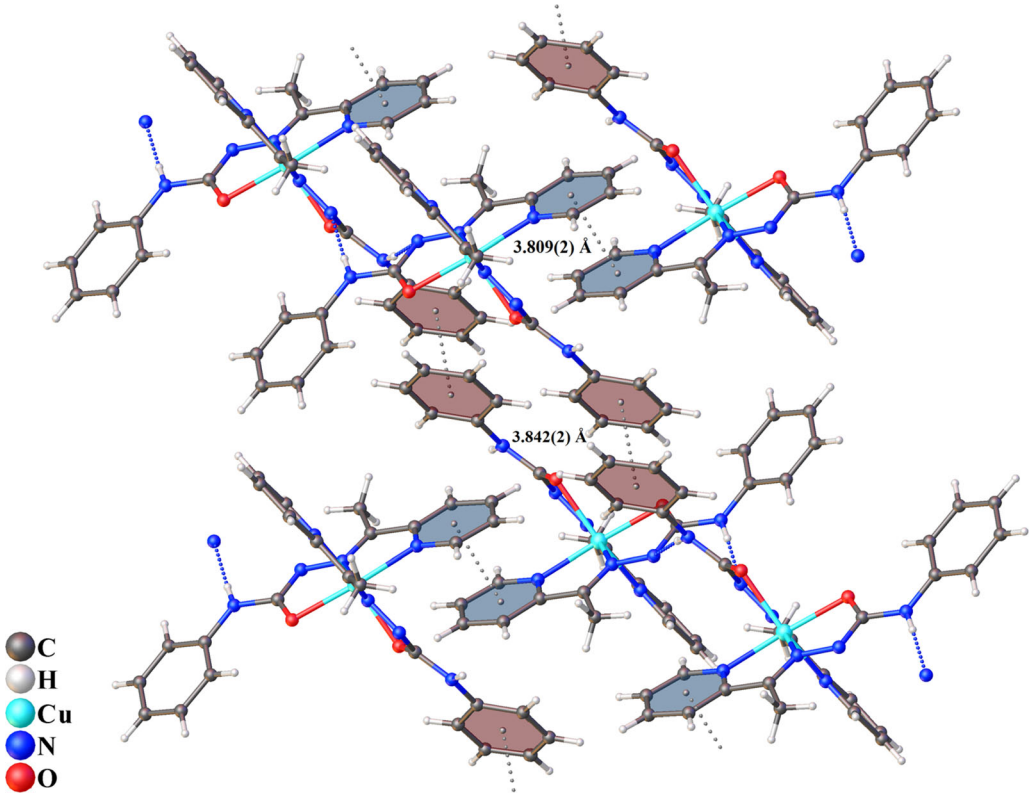

Figure 7. Perspective view of **(6)** showing the chain made up of π···π stacking interactions and hydrogen bonds.

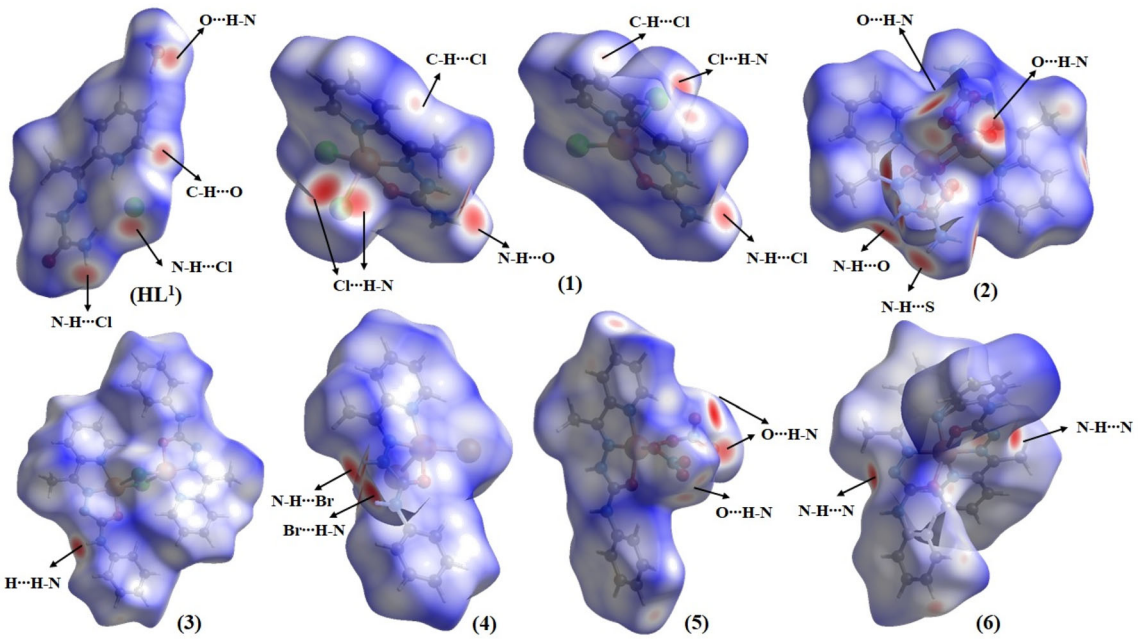

Figure 8. Hirshfeld surface mapped in d_{norm} for $\mathbf{HL^1}$ and **(1–6)**.

Interestingly, the deprotonated nitrogen atoms support the formation of a one-dimensional network of hydrogen bonds that stabilizes the crystal lattice (Figure S6 in SI). The phenyl and pyridyl ring of the complex **(6)** show π···π stacking interactions with centroid-centroid distances of 3.809(2) Å and 3.842(2) Å and promote the formation of a zigzag architecture in the crystal lattice (Figure 7). Selected

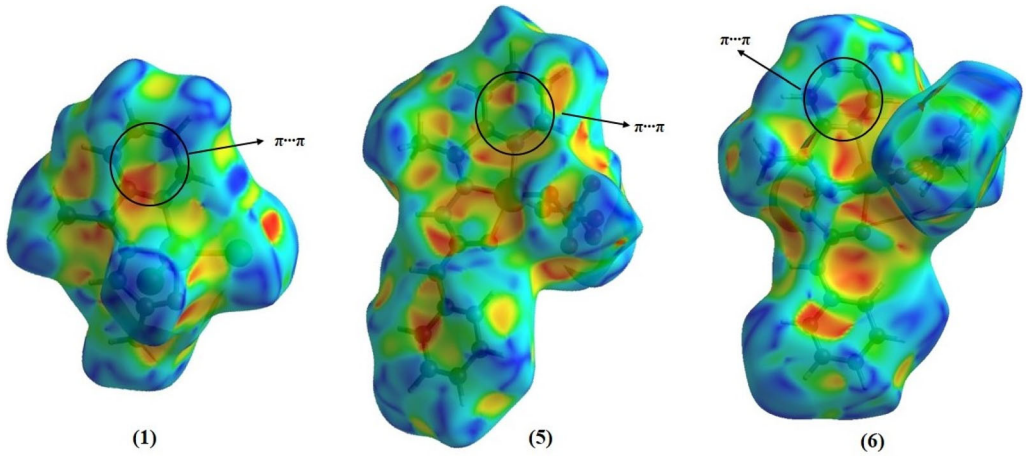

Figure 9. Shape index of **(1)**, **(5)** and **(6)** indicating the presence of π···π stacking interaction.

bond distances and bond angles from the complexes **(3–6)** are listed in Table S3 (SI).

3.3 *Hirshfeld Surface*

To investigate and analyzed the noncovalent interactions in the crystal lattices of the ligand and the copper(II) complexes, the Hirshfeld surface (HS) was used.[30,31] The HS of HL^1 and the metal complexes are shown in Figures 8. The d_{norm} surface exhibits regions with white, blue and red, these colors represent contacts with larger, closer and smaller distances to the sum of van der Waals radii of the atoms, respectively. Red spots can be observed verification the d_{norm} surface, indicating the presence of several close-contacts. The π···π stacking interactions in the crystal structure of the complexes **(1)**, **(5)** and **(6)** are indicate by red and blue triangles in the shape index surface (Figure 9). The fingerprint plots of the compounds indicate that the H···H interaction have the most contribution for HL^1 and the metal complexes **(1)**, **(3)**, **(4)** and **(6)**, with interactions contributed between 25.4% and 54.1%. The H···O interactions have the most contribution for the metal complexes **(2)** and **(5)**, with interactions contributed of 26.3% and 27.1% respectively. The full 2D fingerprint plots of the compounds are in the Figure S19 (SI) and show the total contributions of each noncovalent interactions.

4. Conclusions

In this work we have synthesized a new ligand and six copper(II) complexes of semicarbazone derivatives. The X-ray crystal analyses and the spectral characterization show HL^1 ligand in ketone tautomer with *E* configuration. The difference in the R groups of the semicarbazones and the copper salt starting reagent led to different and interesting crystal structures of the complexes. Among these, complexes **(1)**, **(4)**, **(5)** and **(6)** were shown as mononuclear based structures, while complexes **(2)** and **(3)** were described as dimers. The detailed analysis of the crystal structures showed the excellent coordinating ability of the semicarbazones and their aromatic systems to form π···π interactions.

Supplementary Information (SI)

Crystallographic data for the structures in this work has been deposited at the Cambridge Crystallographic Data Centre, CCDC 1507092-1507098. Copies of this information are available on request at free of charge from CCDC, Union Road, Cambridge, CB21EZ, UK (fax: +44-1223-336-033; e-mail: deposit@ccdc.ac.uk or http://www.ccdc.cam.ac.uk). ^{1}H and ^{13}C NMR spectra of the ligands, FT-IR, figures with crystallographic network formed by interactions, tables with selected bond distances and bond angles, fingerprint plots of the ligand and complexes are available at www.ias.ac.in/chemsci.

Acknowledgements

Financial support received from FAPDF (Process No. 0193.001545/2017). The authors wish to thank for Coordenação de Aperfeiçoamento de Pessoal de Nível Superior—Brasil (CAPES)—Finance Code 001 for fellowships, UnB, FINEP/CTINFRA and FAPDF.

References

1. Pal R, Kumar V, Gupta A and Beniwal V 2014 Synthesis, Characterization and DNA Photocleavage

Study of a Novel Dehydroacetic Acid Based Hydrazone Schiff's Base and Its Metal Complexes *Med. Chem. Res.* **23** 3327
2. Padhyé S and Kauffman G B 1985 Transition Metal Complexes of Semicarbazones and Thiosemicarbazones *Coord. Chem. Rev.* **63** 127
3. Abu-Dief A M and Mohamed I M A 2015 A Review on Versatile Applications of Transition Metal Complexes Incorporating Schiff Bases *Beni-Suef Univ. J. Basic Appl. Sci.* **4** 119
4. Casas J S, García-Tasende M S and Sordo J 2000 Main Group Metal Complexes of Semicarbazones and Thiosemicarbazones. A Structural Review *Coord. Chem. Rev.* **209** 197
5. Beraldo H 2004 Semicarbazonas e Tiossemicarbazonas: O Amplo Perfil Farmacológico e Usos Clínicos *Quim. Nova*. **27** 461
6. Beraldo H and Gambinob D 2004 The Wide Pharmacological Versatility of Semicarbazones, Thiosemicarbazones and Their Metal Complexes *Mini-Rev. Med. Chem.* **4** 31
7. More M S, Joshi P G, Mishra Y K and Khanna P K 2019 Metal Complexes Driven from Schiff Bases and Semicarbazones for Biomedical and Allied Applications: A Review *Mater. Today Chem.* **14** 100195
8. Salem N M H, Rashad A R, El Sayed L, Foro S, Haase W and Iskander M F 2015 Synthesis, Characterization, Molecular Structure and Supramolecular Architectures of Some Copper(II) Complexes Derived from Salicylaldehyde Semicarbazone *Inorg. Chim. Acta* **432** 231
9. Shaabani B, Khandar A A, Mahmoudi F, Maestro M A, Balula S S and Cunha-Silva L 2013 Novel Binuclear Cu(II) Complexes Combining a Semicarbazone Schiff Base with Distinct Bridging Ligands: Structure and Antimicrobial Activity *Polyhedron* **57** 118
10. Abdolhi N, Aghaei M, Soltani A, Mighani H, Ghaemi E A, Javan M, Khalaji A, Sharbati S, Shafipour M and Balakheyli H 2019 Synthesis and Antibacterial Activities of Novel Hg(II) and Zn(II) Complexes of Bis(Thiosemicarbazone) Acenaphthenequinone Loaded to MWCNTs *J. Struct. Chem.* **60** 845
11. Muleta F, Alansi T and Eswaramoorthy R 2019 A Review on Synthesis, Characterization Methods and Biological Activities of Semicarbazone, Thiosemicarbazone and Their Transition Metal Complexes *J. Nat. Sci. Res.* **9** 33
12. Cavalcanti de Queiroz A, Alves M A, Barreiro E J, Lima L M and Alexandre-Moreira M S 2019 Semicarbazone Derivatives as Promising Therapeutic Alternatives in Leishmaniasis *Exp. Parasitol.* **201** 57
13. Todorović T R, Vukašinović J, Portalone G, Suleiman S, Gligorijević N, Bjelogrlić S, Jovanović K, Radulović S, Anđelković K, Cassar A, Filipović N R and Schembri-Wismayer P 2017 (Chalcogen)Semicarbazones and Their Cobalt Complexes Differentiate HL-60 Myeloid Leukaemia Cells and Are Cytotoxic towards Tumor Cell Lines *MedChemComm* **8** 103
14. Machado I, Fernández S, Becco L, Garat B, Gancheff J S, Rey A and Gambino D 2014 New Fac-Tricarbonyl Rhenium(I) Semicarbazone Complexes: Synthesis, Characterization, and Biological Evaluation *J. Coord. Chem.* **67** 1835
15. Santini C, Pellei M, Gandin V, Porchia M, Tisato F and Marzano C 2014 Advances in Copper Complexes as Anticancer Agents *Chem. Rev.* **114** 815
16. Qi J, Liang S, Gou Y, Zhang Z, Zhou Z, Yang F and Liang H 2015 Synthesis of Four Binuclear Copper(II) Complexes: Structure, Anticancer Properties and Anticancer Mechanism *Eur. J. Med. Chem.* **96** 360
17. Venkatachalam T K, Bernhardt P V, Noble C J, Fletcher N, Pierens G K, Thurecht K J and Reutens D C 2016 Synthesis, Characterization and Biological Activities of Semicarbazones and Their Copper Complexes *J. Inorg. Biochem.* **162** 295
18. Marzano C, Pellei M and Santini F T 2009. Copper Complexes as Anticancer Agents *Anticancer Agents Med. Chem.* **9** 185
19. Murphy B and Hathaway B 2003 The Stereochemistry of the Copper(II) Ion in the Solid-State—Some Recent Perspectives Linking the Jahn–Teller Effect, Vibronic Coupling, Structure Correlation Analysis, Structural Pathways and Comparative X-Ray Crystallography *Coord. Chem. Rev.* **243** 237
20. Duncan C and White A R 2012 Copper Complexes as Therapeutic Agents *Metallomics* **4** 127
21. Tiago F S, Santiago P H O, Amaral M M P, Martins J B L and Gatto C C 2016 New Cu(II) Complex with Acetylpyridine Benzoyl Hydrazone: Experimental and Theoretical Analysis *J. Coord. Chem.* **69** 330
22. Gatto C C, Miguel P M, Almeida C M, Santiago P H O, Paier C R K and Pessoa C 2017 A Copper(II) Complex of a Semicarbazone: Crystal Structure, Spectroscopic Analysis and Cytotoxicity against Human Cancer Cell Lines *Transit. Met. Chem.* **42** 503
23. Pérez-Rebolledo A, Piro O, Castellano E E, Teixeira L R, Batista A A and Beraldo H 2006 Metal Complexes of 2-Benzoylpyridine Semicarbazone: Spectral, Electrochemical and Structural Studies *J. Mol. Struct.* **794** 18
24. Gatto C C, Lima I J and Chagas M A S 2017 Supramolecular Architectures and Crystal Structures of Gold(III) Compounds with Semicarbazones *Supramol. Chem.* **29** 296
25. Sheldrick G M 1997 SADABS, Program for Empirical Absorption Correction of Area Detector Data: University of Göttingen: Germany. SHELXS-97. Program for Crystal Structure Resolution. University of Göttingen, Göttingen: Germany 1997
26. Sheldrick G M 1997 SHELXS-97. Program for Crystal Structure Resolution.University of Göttingen, Göttingen, Germany. Program for Empirical Absorption Correction of Area Detector Data: University of Göttingen: Germany 1997
27. Sheldrick G M 2015 Crystal Structure Refinement with SHELXL *Acta Crystallogr. Sect. C Struct. Chem.* **71** 3
28. Farrugia L J 1997 Programa de Representação Das Elipsóides Da Estrutura Cristalina. *Appll. Crystalogr.* **30** 565
29. Farrugia L J 2012 WinGX and ORTEP for Windows: An Update *J. Appl. Crystallogr.* **45** 849
30. Spackman M A and McKinnon J J 2002 Fingerprinting Intermolecular Interactions in Molecular Crystals *CrystEngComm* **4** 378
31. Spackman M A and Jayatilaka D 2009 Hirshfeld Surface Analysis *CrystEngComm* **11** 19

32. Turner M J, McKinnor J J, Wolff S K, et al 2017 *CrystalExplorer17* 2017
33. Siji V L, Kumar M R S, Suma S and Kurup M R P 2010 Synthesis, Characterization and Physiochemical Information, along with Antimicrobial Studies of Some Metal Complexes Derived from an ON Donor Semicarbazone Ligand *Spectrochim. Acta Part A* **76** 22
34. Gil-García R, Fraile R, Donnadieu B, Madariaga G, Januskaitis V, Rovira J, González L, Borrás J, Arnáiz F J and García-Tojal J 2013 Desulfurization Processes of Thiosemicarbazonecopper(Ii) Derivatives in Acidic and Basic Aqueous Media *New J. Chem.* **37** 3568
35. Gil-García R, Ugalde M, Busto N, Lozano H J, Leal J M, Pérez B, Madariaga G, Insausti M, Lezama L, Sanz R, Gómez-Sainz L M, García B and García-Tojal J 2016 Selectivity of a Thiosemicarbazonatocopper(Ii) Complex towards Duplex RNA. Relevant Noncovalent Interactions Both in Solid State and Solution *Dalton Trans.* **45** 18704
36. Kunnath R J, Sithambaresan M, Aravindakshan A A, Natarajan A, Kurup M R P 2016. The Ligating Versatility of Pseudohalides like Thiocyanate and Cyanate in Copper(II) Complexes of 2-Benzoylpyridine Semicarbazone: Monomer, Dimer and Polymer *Polyhedron* **113** 73
37. Gil-García R, Gómez-Saiz P, Díez-Gómez V, Donnadieu B, Insausti M, Lezama L and García-Tojal J 2013 Polymorphism and Magnetic Properties in Thiosemicarbazonecopper(II)-Sulfate Compounds *Polyhedron* **54** 243
38. Garbelini E R, Hörner M, Boneberger Behm M, Evans D J and Nunes F S 2008 Synthesis and Crystal Structures of Bis(1-{(E)-2-Pyridinylmethylidene}-Semicarbazone)Iron(II) and -Copper(II) Diperchlorate Monohydrates *Z. Anorg. Allg. Chemie*. **634** 1801
39. Addison A W, Rao T N, Reedijk J, van Rijn J and Verschoor G C 1984 Synthesis, Structure, and Spectroscopic Properties of Copper(II) Compounds Containing Nitrogen-Sulphur Donor Ligands; the Crystal and Molecular Structure of Aqua[1,7-Bis(N-Methylbenzimidazol-2[Prime or Minute]-Yl)-2,6-Dithiaheptane]Copper(II) Perchlorate *J. Chem. Soc. Dalton Trans.* **7** 1349
40. Senthil Raja D, Bhuvanesh N S P and Natarajan K 2011 Effect of N(4)-Phenyl Substitution in 2-Oxo-1,2-Dihydroquinoline-3-Carbaldehyde Semicarbazones on the Structure, DNA/Protein Interaction, and Antioxidative and Cytotoxic Activity of Cu(II) Complexes *Inorg. Chem.* **50** 12852
41. Layana S R, Saritha, S R, Anitha L, Sithambaresan M, Sudarsanakumar M R and Suma S 2018 Synthesis, Spectral Characterization and Structural Studies of a Novel O, N, O Donor Semicarbazone and Its Binuclear Copper Complex with Hydrogen Bond Stabilized Lattice *J. Mol. Struct.* **1157** 579
42. Lee W Y, Lee P P F, Yan Y K and Lau M 2010 Cytotoxic Copper(Ii) Salicylaldehyde Semicarbazone Complexes: Mode of Action and Proteomic Analysis *Metallomics* **2** 694
43. Todorović T, Grubišić S, Pregelj M, Jagodič M, Misirlić-Denčić S, Dulović M, Marković I, Klisurić O, Malešević A, Mitić D, Anđelković K and Filipović N 2015 Structural, Magnetic, DFT, and Biological Studies of Mononuclear and Dinuclear CuII Complexes with Bidentate N-Heteroaromatic Schiff Base Ligands *Eur. J. Inorg. Chem.* **2015** 3921
44. Patel R N, Shukla K K, Singh A, Choudhary M, Chauhan U K and Dwivedi S 2009 Copper(II) Complexes as Superoxide Dismutase Mimics: Synthesis, Characterization, Crystal Structure and Bioactivity of Copper(II) Complexes *Inorg. Chim. Acta* **362** 4891
45. Chumakov Y M, Tsapkov V I, Antosyak B Y, Bairac N N, Simonov Y A, Bocelli G, Pahontu E and Gulea A P 2009 Crystal Structures of Copper(II) Nitrate, Copper(II) Chloride, and Copper(II) Perchlorate Complexes with 2-Formylpyridine Semicarbazone *Crystallogr. Rep.* **54** 455
46. Leovac V M, Novaković S B, Bogdanović G A, Joksović M D, Mészáros Szécsényi K and Češljević V I 2007 Transition Metal Complexes with Thiosemicarbazide-Based Ligands. Part LVI: Nickel(II) Complex with 1,3-Diphenylpyrazole-4-Carboxaldehyde Thiosemicarbazone and Unusually Deformed Coordination Geometry *Polyhedron* **26** 3783